International Journal of Natural Resource Ecology and Management
2022; 7(1): 15-21
http://www.sciencepublishinggroup.com/j/ijnrem
doi: 10.11648/j.ijnrem.20220701.13
ISSN: 2575-3088 (Print); ISSN: 2575-3061 (Online)

Modelling and Mapping Forest Above-Ground Biomass Using Earth Observation Data

Sami Dawood Madundo*, Ernest William Mauya, Nandera Juma Lolila, Hadija Ahmed Mchelu

Department of Forest Engineering and Wood Sciences, Sokoine University of Agriculture, Morogoro, Tanzania

Email address:

sdmadundo@gmail.com (S. D. Madundo)

*Corresponding author

To cite this article:

Sami Dawood Madundo, Ernest William Mauya, Nandera Juma Lolila, Hadija Ahmed Mchelu. Modelling and Mapping Forest Above-Ground Biomass Using Earth Observation Data. *International Journal of Natural Resource Ecology and Management*. Vol. 7, No. 1, 2022, pp. 15-21. doi: 10.11648/j.ijnrem.20220701.13

Received: January 25, 2022; **Accepted**: February 16, 2022; **Published**: February 25, 2022

Abstract: Accurate information on above-ground biomass (AGB) is important for sustainable forest management as well as for global initiatives aimed at combating climate change in the Tropics. In this study, AGB was estimated using a combination of field and Sentinel-2 earth observation data. The study was conducted at Magamba Nature Reserve in Lushoto district, Tanzania. Field plot-based AGB values were regressed against eighteen Sentinel-2 remote sensing variables (bands and vegetation indices) using Random Forest (RF) models based on centroid and weighted approaches. Results showed that the weighted model had the highest fit and precision (pseudo-R^2 = 0.21, rRMSE = 68.23%). A prediction map was produced with a mean AGB of 223.47 Mg ha^{-1} which was close to that of the field (225.19 Mg ha^{-1}). Furthermore, the standard deviation of the AGB obtained from the map (i.e 174.04 Mg ha^{-1}) was relatively lower as compared to the one obtained from the field-based measurements (i.e 97.42 Mg ha^{-1}). This study demonstrated that Sentinel-2 imagery and RF-based regression techniques have potential to effectively support large scale estimation of forest AGB in the tropical rainforests.

Keywords: Above-ground Biomass, Earth Observation Data, Modelling, Random Forest, Sentinel-2

1. Introduction

Accurate forest above-ground biomass (AGB) retrieval is often required to assist in carbon monitoring, reporting, and verification (MRV) schemes for the global climate change mitigation strategies. One notable mitigation strategy under the United Nations Framework Convention on Climate Change (UNFCCC) is Reducing Emissions from Deforestation and Forest Degradation (REDD+) [1]. In context to this, field-based methods or forest inventory approaches had been considered over time as the most accurate approach for estimating forest AGB [4]. However, this conventional method is associated with limitations related to high cost of field measurements, time-consuming nature, and site selection biases [14]. Furthermore, in the tropical montane forests, accurately mapping and estimation of AGB using field-based methods remains a challenge due to the complex forest structure and topography [12, 32]. Therefore, the development of timely, precise, and cost-effective methods which integrate field and remote sensing-based data is apparently important for monitoring large scale forest AGB in such biomes.

Earth observation through satellite remote sensing has become an appropriate tool for estimating AGB across challenging forest ecosystems [15]. These techniques have the ability to produce accurate estimates and additionally map and monitor the spatial distribution of AGB unlike conventional methods [2, 29]. Earth observation techniques, particularly those based on remotely sensed data, can aid in the ability of obtaining continuous and repetitive digital data from the same location, with varying spatial resolutions, covering extensive areas and reducing processing time as well as costs [22].

Copernicus' twin satellite by the name of Sentinel-2 has a number of specialties essential for land monitoring and assessing bio-geophysical parameters such as AGB [9] particularly in dense forests [11, 13]. This is in part due to the robustness of the Sentinel-2 red-edge bands [28]. In Tanzania, attempts to estimate AGB of plantation forests were done in 2013 by [23] using Landsat products, and in

2019, [25] used ALOS-PALSAR, Sentinel-1 (SAR) and Sentinel-2 as well as their combinations. Thus, very little is known on the prediction and estimation of natural forests AGB based on Sentinel-2 satellite imagery in the country which potentially can support forest carbon monitoring initiatives under REDD+ programmes. This study therefore aims to use this opportunity to explore the capability of using Sentinel-2 satellite imagery in estimating the AGB of a dense natural forest in North-eastern Tanzania. Specifically, the study aimed at 1) to model AGB using spectral bands and indices, 2) to compare the precision of AGB models developed from the Sentinel-2 variables extracted via centroid and area weighted mean approaches, and 3) to estimate and map AGB using Sentinel-2 data.

2. Materials and Methods

2.1. Study Area

The study was conducted at Magamba Nature Reserve, Lushoto district, Tanzania. The forest lies between 4°37'S, 38°11'E and 4°470'S, 38°20'E (Figure 1). The area is characterized by cool climate throughout the year with two distinct rainy seasons [7]. The topography is highly variable ranging from gentle plains to very steep sloping mountainous areas [27].

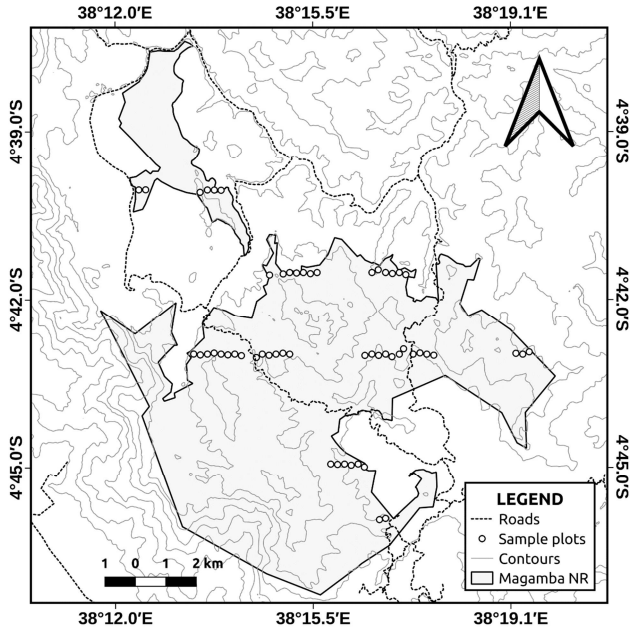

Figure 1. *Location of the study area.*

2.2. Sampling Design

Two phase sampling design was used to establish 55 circular (15 m radius) field sample plots in the forest reserve. The area was initially populated with first-phase sample plots along a grid of 450 by 900 m. Second-phase sample plots were then picked out of the first phase samples based on accessibility and cost. The plot coordinates of the second phase sample plots were then loaded into a global positioning system (GPS) receiver, which were then used to navigate to the actual field plot center locations.

2.3. Field Measurement

All trees with a diameter at breast height (DBH) ≥ 5 cm in each plot were measured using a caliper or diameter tape (depending on the trees' size). In each plot, three trees having the smallest, middle and largest DBH were selected as sample trees for height measurement using a Vertex hypsometer. For trees without height measurements, height was predicted using a height-diameter (H-d) model constructed from the sample trees. The AGB of each individual tree was calculated using allometric models for lowland and humid montane forests developed by [24]. The AGB of all trees within each plot was summed to obtain total AGB for that particular plot and then scaled to per-hectare values according to the respective plot area.

2.4. Satellite Data

Sentinel-2 level 1C multispectral data having ground resolutions of 10, 20 and 60 m was used in this study. The cloud-free image was acquired on 12 March 2019 in the Universal Transverse Mercator (UTM) coordinate system (WGS 84, zone 37S) from the Copernicus Open Access Hub (https://scihub.copernicus.eu). Radiometric correction to bottom-of-atmosphere (BOA) reflectance was performed using the ATCOR algorithm in Sen2Cor [21]. All spectral bands (Appendix 1), with the exception of bands 1 (coastal aerosol), 9 (water vapor) and 10 (SWIR-cirrus), were extracted and reprojected to Arc 1960 UTM/37S coordinate system. Additionally, all bands with more than 10 m were resampled to 10 m resolution to ensure spatial consistency among the bands and maintain the spectral information. Eight selected vegetation indices (Appendix 2) were calculated from the spectral bands to evaluate the potential of the bands operating in the near infra-red (NIR) and red-edge (RE) spectrum [17].

2.5. Data Analysis

This study grouped the analysis into four stages: spectral value extraction, model development, accuracy assessment and AGB mapping. All geospatial and statistical computing was conducted using R version 4.1.2 [30].

2.5.1. Spectral Value Extraction

Two approaches of spectral value extraction were tested (i) a centroid approach where values from the satellite imagery were extracted from a single pixel superimposed with the plot center coordinate, and (ii) a weighted approach in which values were extracted as the weighted mean of the pixels intersecting with the plot area [25].

2.5.2. Model Development

The empirical models relating AGB measured at the plot level and remotely sensed predictor variables were fitted using random forest regression algorithm. Random forest is a non-parametric regression method, which is developed, based

on the regression trees algorithm, where predictor variables are split to grow a number of nodes to select the best predictor variable. About two-thirds of the samples (in-bag samples) are used to train the trees and remaining one third (out-of-bag (OOB) samples) are used in an internal cross-validation technique for estimating the OOB error [18]. The principle behind random forest regression as it is applied in this study is explained in [3] and its use for modelling and prediction of forest tree attributes had widely been reported [11, 16].

A key advantage however, in random forest, is that, greater number of predictor variables of various types (categorical, continuous, binary) can be handled and the relative importance of each predictor variable can be estimated during the model calibration process. Furthermore, RF had the ability to identify complex nonlinear relationships between response and predictor variables [10].

In this analysis, the random forest algorithm was run iteratively using the *randomForest* package in R [20]. The model initially included all covariates, the least influential covariates were dropped, and the model was refitted with six best covariates as per the variable importance figures. The preliminary analysis suggested that the six covariates were most effective for developing a robust model with reasonable prediction accuracy. The importance of each covariate in the model was determined using the *ggRandomForest* package in R [8]. This was essentially aimed to understand how individual predictor variables contribute to the model fit.

2.5.3. Accuracy Assessment

To enable comparison among models with different extraction methods we evaluated the models using the predictions from the internal out of the bag (OOB) sampling procedure, which is equivalent to leave one out cross validation. The predicted values were therefore used to estimate measures of reliability. We used relative root mean square error as the most common statistic used to characterize the error of remote sensing-based forest biomass and volume models. The root mean square error (RMSE) and the relative root mean square error (rRMSE) were calculated as;

$$RMSE = \sqrt{\sum_{i=1}^{n} \frac{(y_i - \hat{y}_i)^2}{n}} \quad (1)$$

and

$$rRMSE = \frac{RMSE}{\bar{y}} \times 100\% \quad (2)$$

where y_i and $\hat{y}_i$ denote field measured AGB and predicted AGB for plot i, respectively, and $\bar{y}$ denotes mean field measured AGB for all plots. The RMSE and the rRMSE were computed based on the predictions from the OOB samples (leave one out cross validation) and compared among the different model categories. Additionally, we also computed pseudo-R^2 as the measure of the quality of the model fit, which was calculated as:

$$pseudo{-}R^2 = 1 - \frac{\sum_{i=1}^{n} (y_i - \hat{y}_i)^2}{\sum_{i=1}^{n} (y_i - \bar{y})^2} \quad (3)$$

2.5.4. AGB Mapping

In order to develop an AGB prediction map, the AGB model with the lowest rRMSE obtained from either centroid or weighted value extraction approach was used to spatially predict AGB over the entire forest area. Furthermore, the descriptive statistics of the AGB prediction map were computed and compared with the field-based estimates.

3. Results

3.1. Field Above-ground Biomass

AGB in different DBH classes showed a reverse trend to that of density distribution (Figures 2a and 2b). The mean field AGB was 225.19 Mg ha^{-1}, with minimum and maximum values of 19.05 Mg ha^{-1} and 720.79 Mg ha^{-1}, respectively. The field standard deviation (SD) was 174.04 Mg ha^{-1}. Most plots had AGB values ranging from 100 to 250 Mg ha^{-1}, with relatively fewer plots having AGB values below 100 Mg ha^{-1} and between 250 to 400 Mg ha^{-1}. The least number of plots were found to have AGB values greater than 550 Mg ha^{-1} (Figure 3).

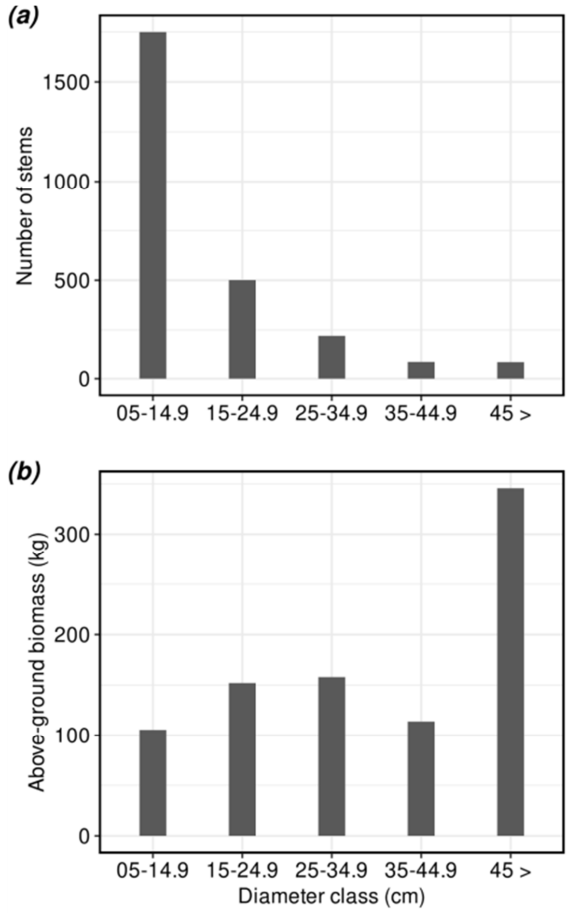

Figure 2. *(a) Density distribution and (b) AGB distribution of trees in the study area.*

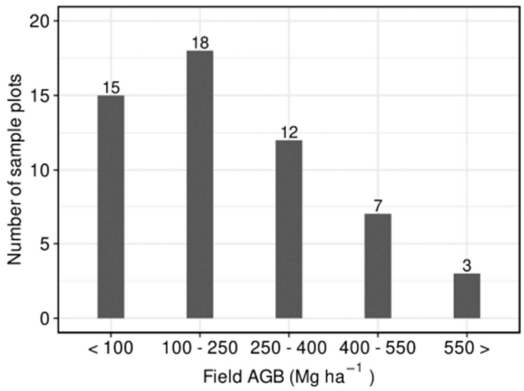

Figure 3. *Distribution of field AGB within the sample plots. The values on top of each bar represents the number of field plots having the given range of field AGB.*

3.2. Variable Selection and Model Performance

The results showed that the AGB models developed from the variables extracted from the weighted-based approach performed relatively better in terms of R^2 and rRMSE as compared to the centroid-based approach (Table 1).

Table 1. *RF model accuracy assessment.*

AGB model	Sentinel-2 spectral data	
	R^2	RMSE%
Centroid	0.096	74.027
Weighted	0.211	68.230

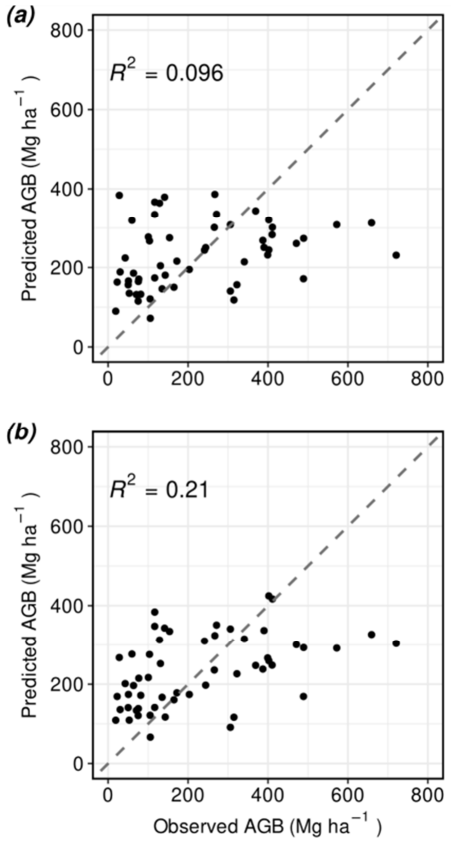

Figure 4. *Predicted vs. observed AGB of sample plots for the (a) centroid-based and (b) weighted-based model.*

The performance of the models for each variable extraction method are further explained with scatter plots (Figure 4) showing the relationships between the field measured AGB and the predicted AGB. The scatter plots indicate that there were obvious overestimation and underestimation problems in the prediction results, no matter which value extraction method was used.

Among the predictor variables, Band 12 (SWIR2) was found to be the most important variable for the weighted-based model (Figure 5). The other most important five predictor variables which were selected were those that are either in a red-edge band or derived from red-edge bands (with the exception of the blue band [B02]).

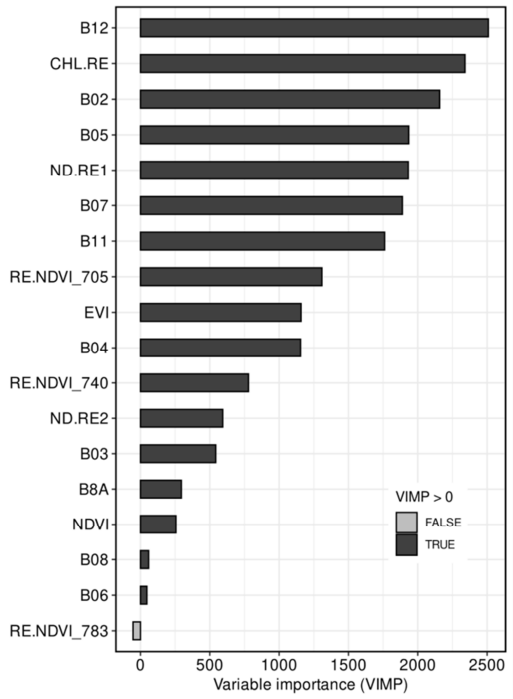

Figure 5. *Random forest predicted variable importance for the weighted-based model showing top variables for AGB prediction.*

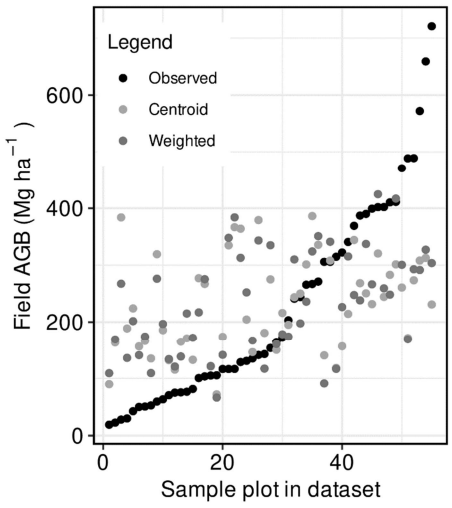

Figure 6. *Comparison of observed AGB and predicted AGB for each model.*

Comparison between the prediction trends of the two models in relation to the observed AGB is shown in Figure 6. Predicted AGB by the weighted model is slightly more consistent with observed field AGB. The AGB of plots containing dense large forest stands with high DBH were likely to be underestimated. Figure 6 also highlights the main limitation of random forest models which is the lack of capacity to predict beyond the range of the response values in the training data, as the highest predicted value of AGB is around the region of 400 Mg ha^{-1}.

3.3. AGB Prediction Map

The identified six Sentinel-2 image predictors as well as the final model were then applied to create an AGB map (Figure 7) of the entire study area. The minimum and maximum predicted AGB was 53.31 and 541.41 Mg ha^{-1} respectively. The mean AGB for the entire nature reserve was 223.47 Mg/ha with a SD of 97.42 Mg ha^{-1}.

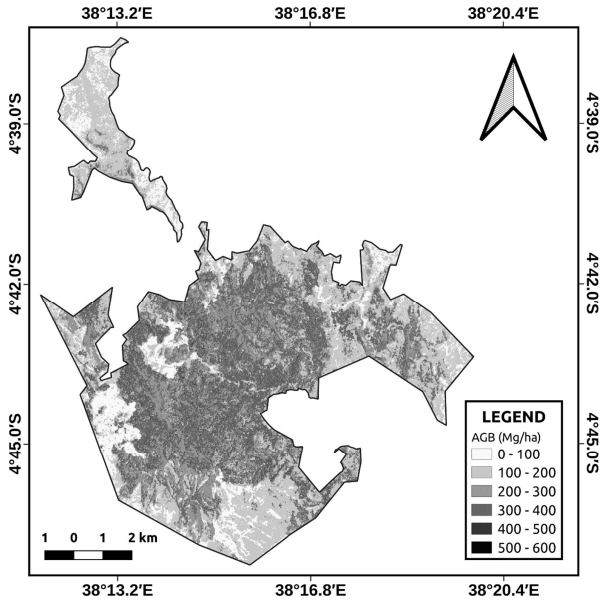

Figure 7. *Spatial distribution of AGB in Magamba nature reserve.*

4. Discussion

The main objective of the study was to determine the potential of Sentinel-2 satellite imagery in modelling, predicting and mapping AGB, and thus investigating the potential of using open-source remotely sensed data to provide information that can support the implementation of REDD+ programme by the UNFCCC in the tropics. This was the first study to be conducted in Tanzania on the estimation of AGB using Sentinel data in a dense tropical mountain forest such as Magamba. As such the study had made a substantial contribution to the field of remote sensing assisted forest inventory.

The results obtained are comparable across the tropical forests with similar vegetation types with slight variations. For example, [28] reported R^2 = 0.81, rRMSE = 25.32% while [6] reported R^2 = 0.81, rRMSE = 36.67%. The reported pseudo-R^2 of 0.21 and rRMSE of 68.23% are generally lower when compared to the other studies mentioned above. However, this is attributed to the more complex forest structure associated with dense crown cover and higher AGB values existing in our study area. Nevertheless, compared to the conventional field-based methods, there is a large substantial gain in terms of more spatial coverage as well as the reduction in the SE of the AGB estimates from 174.04 to 97.42 Mg ha^{-1}. This is evidence of the capability of machine learning techniques, such as Random Forest, in estimating AGB with considerable prediction accuracy.

Among the two approaches of value extraction, the weighted values provided the model with the greatest accuracy in terms of the pseudo-R^2 and rRMSE. This is understandable as weighted values factor in the area covered by the plots and thus result in a more representative pixel value that better relates to AGB as compared to a centroid value approach whose plot centroid may be located in a pixel that shares only part or none of the plot area. This observation is confirmed with findings from [25], irrespective of the value extraction method.

The six important top variables that were selected to develop the final model mostly consisted of SWIR and red-edge band-based variables. This highlights the use of Sentinel-2 data having better spectral (with additional SWIR and red-edge bands) and spatial resolutions among the available medium resolution sensors. SWIR band has shown stronger relations with field measured AGB irrespective of data and environmental settings [26]. Vegetation reflects maximum energy at the NIR region of the electromagnetic spectrum but is unable to provide information on the soil under the vegetation, whereas the SWIR band can differentiate moisture content of vegetation and soil [5]. Therefore, the SWIR band could capture the vegetation cover with the underneath soil conditions more efficiently.

The estimates of AGB for the forest reserve in Magamba are within those reported by [31] for the world's tropical montane forests (i.e., AGB of 77-785 Mg ha^{-1}) as well as those of [19] which was estimated across 260 African tropical forests.

Despite the limitations, the results in this study demonstrated that Sentinel-2 imagery and RF-based regression techniques have potential to effectively support large scale estimation of forest AGB in the tropical rainforests.

5. Conclusion and Recommendation

This study demonstrated an approach for forest AGB estimation by integrating open-source remotely sensed data and field data with the aid of a machine learning algorithm. Random Forest (RF) was applied to identify the dominant spectral bands and vegetation indices to estimate forest AGB. Using a combination of six spectral band and vegetation index variables, the RF algorithm effectively predicted the spatial distribution of forest AGB of Magamba Nature Forest Reserve, Lushoto, Tanga, Tanzania. The method provides a scientific basis for estimating high-resolution forest AGB integrating field data and Sentinel-2 remote sensing data with the help of machine learning techniques. The methodology can be adopted

for mapping and monitoring the forest biomass of Tanzania. This approach can also be used to study the spatio-temporal changes of biomass as it is time and cost-effective. The estimated spatial distribution of AGB is not only an important source for monitoring biomass or carbon stocks, it also contributes to the preparation of national reference scenarios of biomass and implementation of REDD+ activities.

The precision of the forest AGB estimation may be further enhanced by exploiting information from combining both radar and optical multi-source remote sensing data, this can be the potential direction for future studies.

Acknowledgements

The authors acknowledge the Swedish International Development Cooperation Agency, through the postdoctoral program under the Tanzania Commission for Science and Technology for providing the financial support for this study. Additional support was obtained from the Eastern Arc Mountains Conservation Endowment Fund. Lastly the authors are grateful to Tanzania Forest Services Agency (TFS) - Lushoto as well as the Conservator of Magamba Nature Forest Reserve for facilitating all logistics pertaining to field data collection.

Appendix

Appendix 1: Sentinel-2 Spectral Bands

Table 2. *Sentinel-2 Multi-Spectral Instrument (MSI) bands and spatial resolutions.*

Band number	Spatial resolution (m)
B01 – Coastal aerosol	60
B02 - Blue	10
B03 - Green	10
B04 - Red	10
B05 - Vegetation red-edge 1	20
B06 - Vegetation red-edge 2	20
B07 - Vegetation red-edge 3	20
B08 - Near Infra-red (NIR)	10
B8A - Narrow NIR	20
B09 - Water vapor	60
B10 - SWIR-cirrus	60
B11 - SWIR1	20
B12 - SWIR2	20

Source: ESA (2015).

Appendix 2: Vegetation Indices

Table 3. *Vegetation indices calculated from the Sentinel-2 images.*

Index	Formula
NDVI	(B08 – B04) / (B08 + B04)
EVI	2.5 * (B08 – B04) / (B08 + 6 × B04 – 7.5*B02 + 1)
RE-NDVI 1	(B08 – B06) / (B08 + B06)
RE-NDVI 2	(B08 – B07) / (B08 + B07)
RE-NDVI 3	(B08 – B05) / (B08 + B05)
ND-RE1	(B06 – B05) / (B06 + B05)
ND-RE2	(B07 – B05) / (B07 + B05)
CHL-RE	(B07 – B05) - 1

Source: Mauya *et al.* (2019).

References

[1] Ali, A., Ashraf, M. I., Gulzar, S., and Akmal, M. 2020. Estimation of forest carbon stocks in temperate and subtropical mountain systems of Pakistan: implications for REDD+ and climate change mitigation. Environmental Monitoring and Assessment, 192 (3), 198.

[2] Baccini, A., Laporte, N., Goetz, S. J., Sun, M., and Dong, H. 2008. A first map of tropical Africa's above-ground biomass derived from satellite imagery. Environmental Research Letters, 3 (4), 045011.

[3] Breiman, L. 2001. Random Forest. Machine Learning, 45, 5–32.

[4] Brown, D., Jorgenson, M., Kielland, K., Verbyla, D., Prakash, A., and Koch, J. 2016. Landscape Effects of Wildfire on Permafrost Distribution in Interior Alaska Derived from Remote Sensing. Remote Sensing, 8 (8), 654.

[5] Brown, S. 2002. Measuring carbon in forests: current status and future challenges. Environmental Pollution, 116 (3), 363–372.

[6] Dang, A. T. N., Nandy, S., Srinet, R., Luong, N. V., Ghosh, S., and Senthil Kumar, A. 2019. Forest aboveground biomass estimation using machine learning regression algorithm in Yok Don National Park, Vietnam. Ecological Informatics, 50, 24–32.

[7] Debien, A., Neerinckx, S., Kimaro, D., and Gulinck, H. 2010. Influence of satellite-derived rainfall patterns on plague occurrence in northeast Tanzania. International Journal of Health Geographics, 9 (1), 60.

[8] Ehrlinger, J. 2016. ggRandomForests: Visually Exploring Random Forests. R package version 2.0.1. https://CRAN.R-project.org/package=ggRandomForests.

[9] ESA. 2015. SENTINEL-2 User handbook. European Commission.

[10] Fassnacht, F. E., Hartig, F., Latifi, H., Berger, C., Hernández, J., Corvalán, P., and Koch, B. 2014. Importance of sample size, data type and prediction method for remote sensing-based estimations of aboveground forest biomass. Remote Sensing of Environment, 154, 102–114.

[11] Forkuor, G., Benewinde Zoungrana, J. B., Dimobe, K., Ouattara, B., Vadrevu, K. P., and Tondoh, J. E. 2020. Above-ground biomass mapping in West African dryland forest using Sentinel-1 and 2 datasets - A case study. Remote Sensing of Environment, 236 (November 2018), 111496.

[12] Gemmell, F. M. 1995. Effects of forest cover, terrain, and scale on timber volume estimation with Thematic Mapper data in a rocky mountain site. Remote Sensing of Environment, 51 (2), 291–305.

[13] Ghosh, S. M., and Behera, M. D. 2018. Aboveground biomass estimation using multi-sensor data synergy and machine learning algorithms in a dense tropical forest. Applied Geography, 96 (March), 29–40.

[14] Hall, R. J., Skakun, R. S., Arsenault, E. J., and Case, B. S. 2006. Modeling forest stand structure attributes using Landsat ETM+ data: Application to mapping of aboveground biomass and stand volume. Forest Ecology and Management, 225 (1–3), 378–390.

[15] Hese, S., Lucht, W., Schmullius, C., Barnsley, M., Dubayah, R., Knorr, D., Neumann, K., Riedel, T., and Schröter, K. 2005. Global biomass mapping for an improved understanding of the CO_2 balance—the Earth observation mission Carbon-3D. Remote Sensing of Environment, 94 (1), 94–104.

[16] Hojas Gascón, L., Ceccherini, G., García Haro, F., Avitabile, V., and Eva, H. 2019. The potential of high resolution (5 m) RapidEye optical data to estimate above ground biomass at the national level over Tanzania. Forests, 10 (2), 107.

[17] Imran, A. B., Khan, K., Ali, N., Ahmad, N., Ali, A., and Shah, K. 2020. Narrow band based and broadband derived vegetation indices using Sentinel-2 Imagery to estimate vegetation biomass. Global Journal of Environmental Science and Management, 6 (1), 97–108.

[18] Jafarzadeh, H., Mahdianpari, M., Gill, E., Mohammadimanesh, F., and Homayouni, S. 2021. Bagging and Boosting Ensemble Classifiers for Classification of Multispectral, Hyperspectral and PolSAR Data: A Comparative Evaluation. Remote Sensing, 13 (21), 4405.

[19] Lewis, S. L., Sonké, B., Sunderland, T., Begne, S. K., Lopez-Gonzalez, G., Van Der Heijden, G. M., Phillips, O. L., Affum-Baffoe, K., Baker, T. R. and Banin, L. 2013. Above-ground biomass and structure of 260 African tropical forests. Philosophical Transactions of the Royal Society B: Biological Sciences 368, 20120295.

[20] Liaw, A. and Wiener, M. 2002. Classification and Regression by randomForest. R News 2 (3), 18-22.

[21] Louis, J., Debaecker, V., Pflug, B., Main-Knorn, M., Bieniarz, J., Mueller-Wilm, U., Cadau, E., and Gascon, F. 2016. Sentinel-2 SEN2COR: L2A processor for users. European Space Agency, (Special Publication) ESA SP, SP-740 (May), 9–13.

[22] Lu, D. 2006. The potential and challenge of remote sensing-based biomass estimation. International Journal of Remote Sensing, 27 (7), 1297–1328.

[23] Mahuve, T. G. 2013. Estimation of Forest Aboveground Biomass using Remote Sensing and GIS: A Case Study of a REDD Pilot Project in Lindi Tanzania. Unpublished Dissertation for Award of MSc Degree at Ardhi University, Dar es Salaam, Tanzania.

[24] Masota, A., Bollandsås, O., Zahabu, E. and Eid, T. 2016. 4 Allometric Biomass and Volume Models for Lowland and Humid Montane Forests. Allometric Tree Biomass and Volume Models in Tanzania, 35.

[25] Mauya, E. W., Koskinen, J., Tegel, K., Hämäläinen, J., Kauranne, T., and Käyhkö, N. 2019. Modelling and Predicting the Growing Stock Volume in Small-Scale Plantation Forests of Tanzania Using Multi-Sensor Image Synergy. Forests, 10 (3), 279.

[26] Nandy, S., Singh, R., Ghosh, S., Watham, T., Kushwaha, S. P. S., Kumar, A. S., and Dadhwal, V. K. 2017. Neural network-based modelling for forest biomass assessment. Carbon Management, 8 (4), 305–317.

[27] Neerinckx, S., Peterson, A. T., Gulinck, H., Deckers, J., Kimaro, D., and Leirs, H. 2010. Predicting Potential Risk Areas of Human Plague for the Western Usambara Mountains, Lushoto District, Tanzania. American Journal of Tropical Medicine and Hygiene, 82 (3), 492–500.

[28] Pandit, S., Tsuyuki, S., and Dube, T. 2018. Estimating Above-Ground Biomass in Sub-Tropical Buffer Zone Community Forests, Nepal, Using Sentinel 2 Data. Remote Sensing, 10 (4), 601.

[29] Pham, L. T. H., and Brabyn, L. 2017. Monitoring mangrove biomass change in Vietnam using SPOT images and an object-based approach combined with machine learning algorithms. ISPRS Journal of Photogrammetry and Remote Sensing, 128, 86–97.

[30] R Core Team. 2021. R: A Language and Environment for Statistical Computing. R Foundation for Statistical Computing: Vienna, Austria. http://www.r-project.org/.

[31] Spracklen, D. & Righelato, R. 2014. Tropical montane forests are a larger than expected global carbon store. Biogeosciences 11, 2741-2754.

[32] Southworth, J., and Tucker, C. 2001. The influence of accessibility, local institutions, and socioeconomic factors on forest cover change in the mountains of western Honduras. Mountain Research and Development, 21 (3), 276–283.